# STATISTICAL ESTIMATION OF FADE DEPTH AND OUTAGE PROBABILITY DUE TO MULTIPATH PROPAGATION IN SOUTHERN AFRICA

## Mike O. Asiyo[*] and Thomas J. O. Afullo

Department of Electrical, Electronic and Computer Engineering, University of KwaZulu-Natal, King George V Avenue, Durban 4041, South Africa

**Abstract**—This study builds on the earlier work by Odedina and Afullo on Multipath fading in Durban. Their work was based on multipath measurements in Durban over a 6.73 km Line-of-Sight (LOS) link. This submission uses the geoclimatic factor approach and ITU-R recommendations P530-14 to obtain the multipath fading occurrence in five cities in South Africa, including Durban. Three-year radiosonde data is used in estimating the percentage of time that a certain fade depth is exceeded and hence outage probability due to atmospheric multipath propagation, assuming the given fade depth leads to the received signal falling below the squelch level. We employ the Inverse Distance Square technique to estimate point refractivity gradient not exceeded for 1% of the time in the lowest 65 m above the ground for five locations within South Africa. Standard error of the mean and confidence interval for both annual averages and seasonal averages of point refractivity gradient is calculated to reflect possible deviation in the given readings. These values of point refractivity gradient obtained are used in determining the geoclimatic factor $K$. The results presented show monthly, seasonal and annual variation of both point refractivity gradient and geoclimatic factor $K$. The results confirm that the geoclimatic factor $K$ is region based. The percentage of time a given fade depth is exceeded for a single frequency increases rapidly with increasing path length. This is due to the fact that as the path length increases so do the multiple reflections leading to multipath propagation, which can result in either signal enhancement or multipath fading. A comparison of fade depth and outage probabilities is made with the earlier work in Durban and Rwanda in Central Africa.

\* Corresponding author: Mike Omondi Asiyo (211559880@stu.ukzn.ac.za).

## 1. INTRODUCTION

Terrestrial fixed radio links operating at microwave frequencies on line-of-sight (LOS) paths are flexible, reliable and economical means of providing point-to-point communications. They are heavily employed in carrying large numbers of voice, video, wide-band data transmissions, high quality audio, and high definition TV channels among others [1, 2]. Their performance and availability characteristics must be above a certain threshold in order to offer high quality of service. This calls for high precision equipment and devices in addition to knowledge of the transmission medium. For LOS links, the transmission medium is the troposphere, with varying climatic conditions which affect the propagation of radio waves. Apart from precipitation, multipath propagation is also a major cause of attenuation of transmitted radio waves [1]. Usually, service availability of 99.99% for the worst month is the design target for fixed links; this implies an outage not exceeding 53 minutes in a year [2].

Clear-air fading mechanisms due to extreme refractive layers in the atmosphere include beam spreading, antenna decoupling, surface multipath and atmospheric multipath. These mechanisms can occur by themselves and/or in combination with each other. A more severe multipath fading occurs when the direct beam spreading of the signal combines with the surface reflected beam [3]. Multipath fading is due to changes in the atmosphere which are of themselves random, hence, the prediction of fading occurrence and/or distribution can only be described by statistical methods. ITU-R [3] provides techniques for estimating the percentage of time that a fade depth is exceeded in the average worst month. It further recommends prediction methods based on specific climatic and topographical conditions. Region-based techniques for deep fading predictions have been available for a number of countries for several years. They include the Barnet-Vigants model for United States and the Morita model for Japan, among others [4–6].

These techniques for predicting the percentage of time that a certain fade depth is exceeded are a function of frequency, path length and geoclimatic factor, with the ITU-R method having an additional variable of path inclination. The ITU-R suggests that region-based methods are likely to be more accurate than the ITU-R technique in the estimation of percentage of time of fade depth exceeded in the worst month because of the effect of the geoclimatic factor. They further recommend that in determining the geoclimatic factor, fading data in the region of interest should be used in the estimation. However, where fading data is not available, it provides a procedure of estimating the geoclimatic factor based on refractivity gradients in the region of

interest [3].

In this paper, the probability that a fade depth of a certain magnitude will occur and hence the probability of outage is estimated based on the effect of the geoclimatic factor derived from atmospheric refractivity gradient. The refractivity gradient is estimated from the radiosonde data obtained from South Africa Weather Service (SAWS). The radiosonde soundings are usually made twice per day and allow for estimation of vertical refractivity profiles derived from their temperature, pressure and humidity measurements. However, radiosonde data suffer from two major drawbacks; poor spatial resolution and lack of time resolutions, hence the data has limited capability to represent diurnal variation [7, 8]. Surface measurements from stations give a better resolution than radiosonde sounding, more so in space. Diurnal patterns can be achieved from surface data taken three to four times a day. The limitation here is lack of values above the surface for vertical refractivity profile approximations. This drawback can be minimized by use of sensors positioned at ground level for surface measurements and at specific altitudes above the ground from which radio refractivity and refractivity gradients can be determined [7]. When a number of stations need to be considered then the cost of the latter method rises tremendously. This leaves the radiosonde soundings as the best bargain for radioclimatic analysis supported with validation schemes for the resulting data.

The rest of this paper is organized as follows: Section 2 presents geographical description of the region under study. Spatial technique applied in estimating the point refractivity gradient is described in Section 3 with Section 4 explaining the steps in determination of geoclimatic factor $K$. Section 5 outlines the fade depth and outage probability estimation; Section 6 shows the results and discussion, while the conclusion is given in Section 7.

## 2. STUDY AREA

South Africa is located in the southern part of the continent of Africa. It experiences four seasons in a year with a slight variations in the regions. The summer season is from mid-October to mid-February, with hot sunny weather and thunderstorms in the afternoon; with the exception of Western Cape which gets its rain in winter. Autumn is from mid-February to April, winter from May to July and spring coming in from August to mid-October. South Africa is bordered by the Indian Ocean and Atlantic Ocean on the southern part of the country. It is divided into nine regions: Western Cape (with Cape Town as the main city) is typically Mediterranean, with temperature

ranging from 5°C to 22°C. Eastern Cape is mainly Savannah and lies between subtropical climate of KwaZulu Natal and the Mediterranean of Western Cape. Its temperature ranges from 7°C in winter and 26°C in summer. KwaZulu Natal with Durban as the main city is generally warm with temperature ranging from 16°C to 33°C. Gauteng is mainly temperate with mild climate, neither humid nor too hot with Pretoria as the main city. The Northern Province of South Africa is mostly subtropical with Polokwane as the main city. Free State region with Bloemfontein as the main city has Steppe climate with temperature ranging from as low as 1°C in winter to 32°C in summer. North West province forms part of the Kalahari Desert with temperatures from 2°C to 34°C. Mpumalanga is known as a province of two halves; high-lying grassland savannah of the Highveld escarpment and subtropical Lowveld plains. Lastly, the Northern Cape is mainly semi desert with a small section of Green Kalahari [9–11]. Figure 1 shows the map of South Africa and the bordering countries of Botswana, Namibia, Lesotho and Swaziland [12].
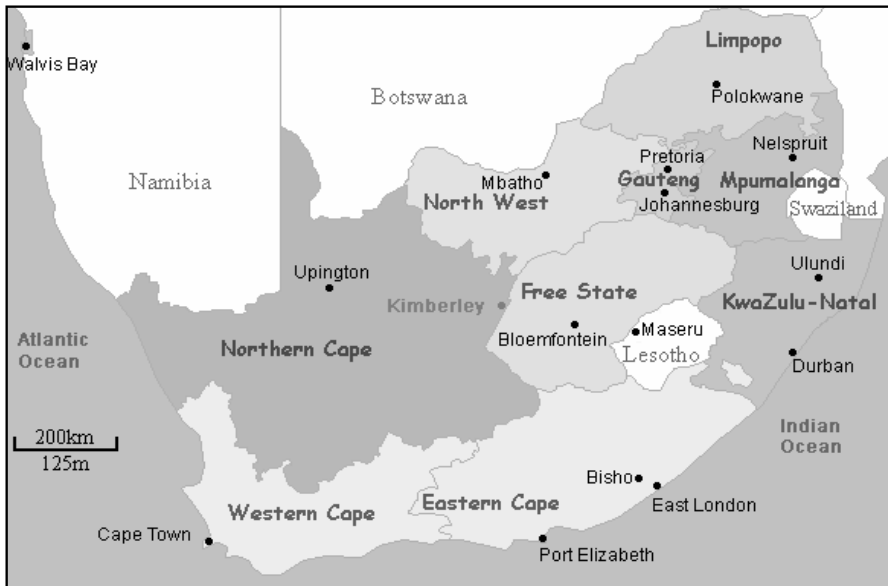


**Figure 1.** Map of South Africa [12].

## 3. INVERSE DISTANCE SQUARE (IDS)

Spatial interpolation is a technique used in data analysis to estimate a set of observations related with a set of sampled points or places to a set of un-sampled points or places where observations are not available. The rational with spatial interpolation is that points closer to each other tend to have similar values than those far apart [13]. Estimations of virtually all spatial interpolation techniques can be represented as weighted averages of sampled data and they all share the same general approximation method, as follows [14]:

$$\acute{Z}(x_0) = \sum_{i=1}^{n} \lambda_i Z(x_i) \tag{1}$$

where $\acute{Z}$ is the estimated value of an attribute at the point of interest $x_0$, $Z$ the observed value of the sampled point $x_i$, $\lambda_i$ the weight allocated to the sample point, and $n$ the number of sampled points used for approximation. Techniques that use distance based weighting of the data assume that each datum has a local influence that reduces as the distance increases until a point at which the influence is negligible. The inverse distance weighting or inverse distance weighted (IDW) method estimates the values of an attribute at un-sampled points using a linear addition of values at sampled points weighted by an inverse function of the distance from the point of interest to the sampled points. The weighting bias can be represented by (2), where $d_i$ is the distance between $x_0$ and $x_i$, $p$ a power parameter, and $n$ as defined previously [14]:

$$\lambda_i = \frac{1/d_i^p}{\sum_{i=1}^{n} 1/d_i^p} \tag{2}$$

where

$$\sum_{i=1}^{n} \lambda_i = 1 \tag{3}$$

The main factor influencing the accuracy of IDW is the value of the power parameter, and if $p$ is 2, then the method is called Inverse Distance Square. The other factor influencing the accuracy is the number of sampled points used in estimations which is also chosen arbitrarily [14].

## 4. GEOCLIMATIC FACTOR DETERMINATION

It has been mentioned in Section 1 that the propagation of radio waves in the troposphere is influenced by the variations of climatic conditions

(temperature, pressure and humidity). These parameters are related to the atmospheric refractivity and can be expressed as in (4), where $N$ is the atmospheric refractivity, $n$ is the refractive index of the atmosphere, $T$ is the temperature (K), $P$ is the atmospheric pressure (hpa) and $e$ is the water vapour pressure (hpa) [15, 16]:

$$N = (n - 1) \times 10^6 = \frac{77.6}{T} \left( P + 4810 \frac{e}{T} \right) \qquad (4)$$

The water vapour pressure $e$ is given by (5), where $H$ (%) is the relative humidity and $t$ (°C) is the air temperature [15]:

$$e = \frac{6.1121H}{100} \exp \left( \frac{17.502t}{t + 240.97} \right) \qquad (5)$$

The refractivity gradient which is a measure of how refractivity varies with height is of greater interest to the LOS link designers. Multipath fading can only occur if this refractivity gradient in the atmosphere varies with height [2]. Refractivity gradient is estimated from (6) where $N_1$ and $N_2$ are the refractivity at heights $h_1$ and $h_2$ respectively [17]:

$$\frac{dN}{dh} \approx \frac{N_2 - N_1}{h_2 - h_1} \qquad (6)$$

Frequency of occurrence of refractivity gradient in the first 65 m above the ground is determined. Then cumulative distribution of $dN/dh$ is then determined from the frequency of occurrence. From the cumulative distribution curve, the point refractivity gradient not exceeded for 1% of each of the months is then determined. In case where the 1% of the refractivity gradient is not available from the distribution curves, inverse distance square technique described in the previous section is used to estimate the value from the nearest values. The geoclimatic factor (for quick planning) can be determined from the procedure given in [3], where $dN_1$ is the point refractivity gradient in the lowest 65 m of the atmosphere not exceeded for 1% of an average year; that is [3]:

$$K = 10^{-4.6 - 0.0027 dN_1} \qquad (7)$$

## 5. FADE DEPTH PREDICTION

Fade depth is a ratio, expressed in decibels, of a reference signal power to the signal power during a fade [18]. ITU-R [3] provides methods for estimating narrow-band fading distribution at large fade depths in the average worst month for both quick planning and for detailed planning purposes. They both involve three steps: estimating the geoclimatic factor $K$, then calculating the path inclination and lastly calculating

the percentage of time that a certain fade depth $A$ is exceeded in the average worst month. Geoclimatic factor determination has been described in Section 4 above. Path inclination ($\varepsilon_p$) can be determined from transmit and receive antenna heights $h_e$ and $h_r$ (m), above sea level and the path length $d$ (km) from (8) [3]:

$$|\varepsilon_p| = |h_e - h_r|/d \qquad (8)$$

For quick planning purpose, the third step can then be estimated from (9), where $p_w$ is the percentage of time that fade depth $A$ (dB) is exceeded in the average worst month, $f$ is the frequency (GHz), $h_L$ is the altitude of the lower antenna (the smaller of $h_e$ and $h_r$), $d$ and $K$ are path length and geoclimatic factor, respectively.

$$p_w = K d^{3.1}(1 + |\varepsilon_p|)^{-1.29} f^{0.8} \times 10^{-0.00089h_L - A/10} \qquad (9)$$

Due to the ever varying nature of the propagation medium, the knowledge of the probability of a fade depth of a particular magnitude to occur, will lead directly to the probability of outage and hence the link availability probability, assuming the given fade depth leads to the received signal falling below the squelch level [2]. In this submission, we have used ITU-R method for quick planning which has an overall standard deviation of error in predictions of 5.9 dB. The accuracy in predictions will improve if the ITU-R method for detailed link design, which requires terrain data, were used. The overall standard deviation of error for detailed applications method is 5.7 dB [3].

## 6. RESULTS AND DISCUSSION

### 6.1 Geoclimatic Factor

Radiosonde data collected from SAWS for three years (2004–2006) is used in the analysis. Radiosonde balloons are launched twice per day at around 10 am in the morning and 11pm in the night. However, in some cases in various months data was available only once per day. In some isolated circumstances, data is reported thrice per day hence showing the non-uniformity in the monthly samples used in the analysis. It is worth noting that radiosonde soundings do not report climatic parameters (i.e., temperature, humidity and pressure) at definite heights. Therefore, the value of $dN_1$ is estimated using (6) where $N_1$ is considered at the $h_1$ value nearest to 65 m height, so that $h_1$ falls within $65 \pm 10\%$ m [17]. Generally, for the design of radio communication systems, the essential statistics of the effects of propagation pertain to that of the worst month. The worst month in a year for a preselected threshold for any performance degrading mechanism is that month in a period of the twelve consecutive calendar

months, during which the threshold is exceeded for the longest time. It must also be noted that the worst month is not necessarily the same month for all the threshold levels [19]. Figures 2–6 show monthly variations of point refractivity gradient for the three years and their averages. Results indicate that the worst cases fall in the summer months apart from Cape Town that has the worst cases in winter. This seems to follow the same trend seen in Section 2, where all the regions had their rainy season in summer apart from Cape Town having its rainy season in winter.

Figures 2–6 have shown monthly variation of point refractivity gradient for three years in each of the five locations. Figure 7 shows yearly averages for the point refractivity gradient with corresponding error bars to indicate the confidence intervals of our estimates. The average for the three years is also shown for each of the locations. It's evidenced that point refractivity gradient also varies annually. In our study, the results show that the year 2004 has the lowest value of point refractivity gradient and the value becomes less negative in the succeeding years. The standard error ($SE$) for each year was calculated from: $SE = S = s/\sqrt{n}$, where $s$ is the sample standard deviation and $n$ is the number of samples. From the values of $SE$, confidence intervals ($CI$) which shows the range in which the "true" value of the estimates fall were calculated from: $CI = S = m \pm 1SE$, where $m$ is the mean/average value of point refractivity gradient of each of the years. Monthly variation of point refractivity gradient depends on season with
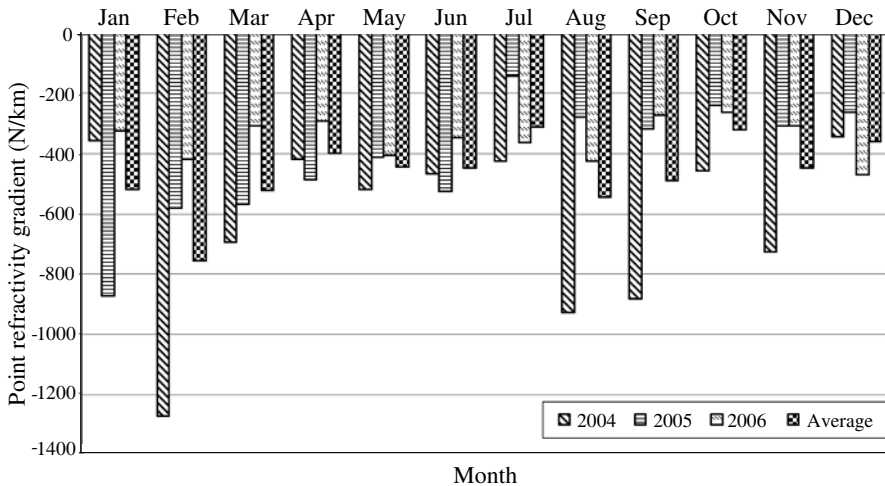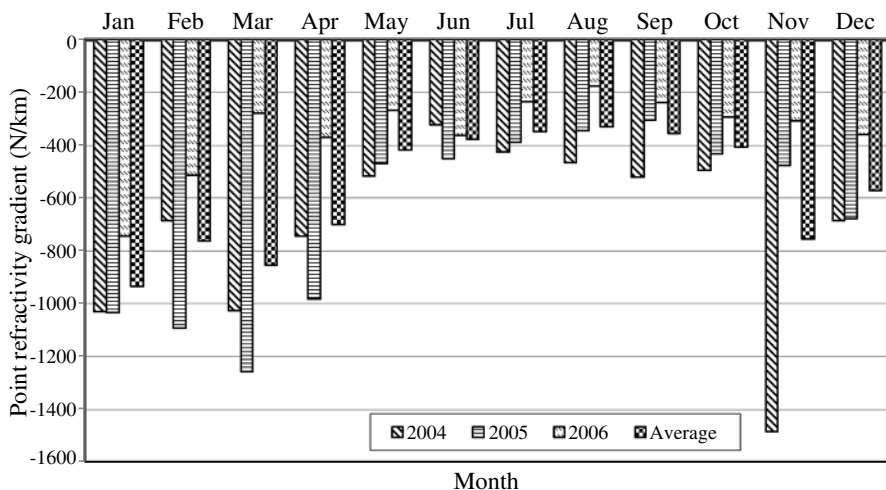


**Figure 2.** Monthly variation of point refractivity gradient in the lowest 65 m of the atmosphere not exceeded for 1% of an average year for Durban.
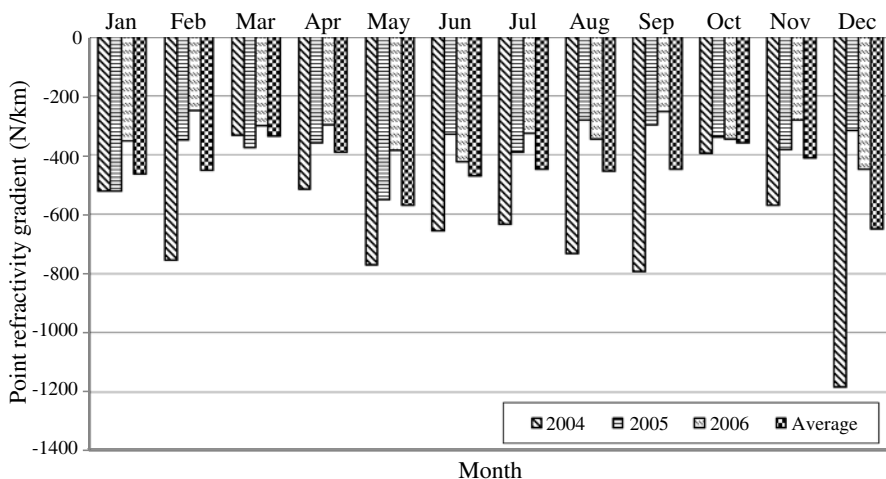
**Figure 3.** Monthly variation of point refractivity gradient in the lowest 65 m of the atmosphere not exceeded for 1% of an average year for Cape Town.
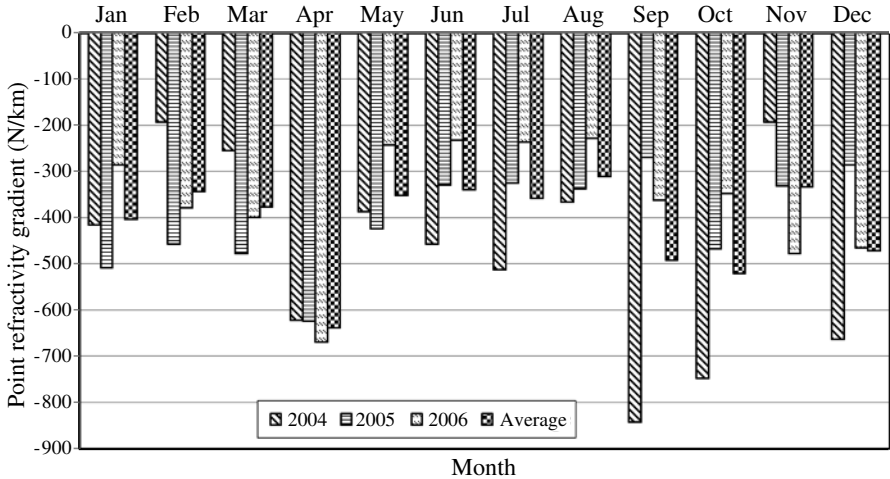


**Figure 4.** Monthly variation of point refractivity gradient in the lowest 65 m of the atmosphere not exceeded for 1% of an average year for Pretoria.

worst months occurring mainly in summer. However, annual variation seems to follow some cycle which needs to be determined and we are processing data for more years to ascertain this hypothesis.

Table 1 provides the summary of the worst month for the

regions with point refractivity gradient values and their corresponding geoclimatic factor $K$ values. Tables 2, 3 and 4 tabulate the values of geoclimatic factor $K$ for each of the months for the three year period under study in the five locations in South Africa. As expected the values of geoclimatic factors are inverse to those of point refractivity gradients. It should be noted that, in estimating the average values of



**Figure 5.** Monthly variation of point refractivity gradient in the lowest 65 m of the atmosphere not exceeded for 1% of an average year for Bloemfontein.
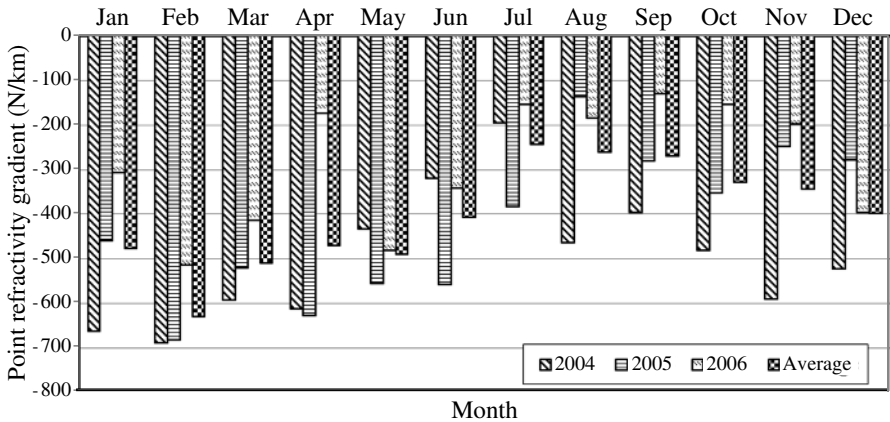


**Figure 6.** Monthly variation of point refractivity gradient in the lowest 65 m of the atmosphere not exceeded for 1% of an average year for Polokwane.

**Table 1.** Worst month values.

|  | Worst Month | Point Refractivity Gradient | Geoclimatic Factor $K$ |
|---|---|---|---|
| Durban | February | $-756.234$ | 2.77E-03 |
| Cape Town | December | $-648.629$ | 1.42E-03 |
| Pretoria | January | $-935.38$ | 8.42E-03 |
| Bloemfontein | April | $-638.324$ | 1.33E-03 |
| Polokwane | February | $-628.676$ | 1.25E-03 |

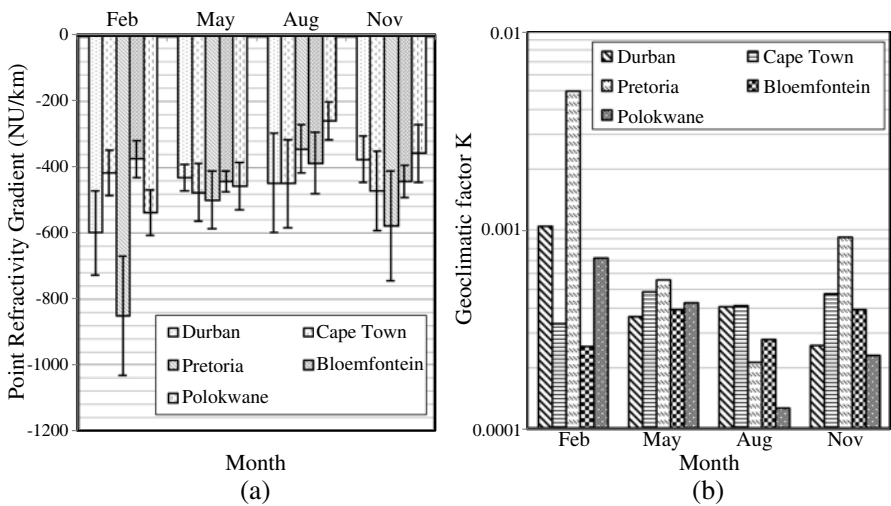**Table 2.** Geoclimatic factor $K$ for Durban and Pretoria.

|  | Durban | | | | Pretoria | | | |
|---|---|---|---|---|---|---|---|---|
|  | 2004 | 2005 | 2006 | Average | 2004 | 2005 | 2006 | Average |
| Jan | 2.31E-04 | 5.66E-03 | 1.88E-04 | 6.27E-04 | 6.35E-04 | 6.44E-04 | 2.55E-03 | 8.42E-03 |
| Feb | 6.82E-02 | 9.22E-04 | 3.36E-04 | 2.77E-03 | 2.71E-03 | 2.18E-04 | 6.06E-04 | 2.87E-03 |
| Mar | 1.86E-03 | 8.58E-04 | 1.70E-04 | 6.48E-04 | 2.00E-04 | 2.56E-04 | 1.41E-04 | 5.07E-03 |
| Apr | 3.39E-04 | 5.19E-04 | 1.56E-04 | 3.01E-04 | 6.17E-04 | 2.32E-04 | 2.51E-04 | 1.93E-03 |
| May | 6.30E-04 | 3.23E-04 | 3.13E-04 | 3.99E-04 | 3.03E-03 | 7.73E-04 | 1.34E-04 | 3.39E-04 |
| Jun | 4.61E-04 | 6.57E-04 | 2.19E-04 | 4.05E-04 | 1.48E-03 | 1.94E-04 | 2.41E-04 | 2.65E-04 |
| Jul | 3.51E-04 | 6.14E-05 | 2.38E-04 | 1.72E-04 | 1.28E-03 | 2.82E-04 | 1.07E-04 | 2.20E-04 |
| Aug | 7.94E-03 | 1.42E-04 | 3.53E-04 | 7.35E-04 | 2.35E-03 | 1.44E-04 | 7.45E-05 | 1.93E-04 |
| Sep | 5.98E-03 | 1.82E-04 | 1.37E-04 | 5.31E-04 | 3.49E-03 | 1.58E-04 | 1.11E-04 | 2.28E-04 |
| Oct | 4.35E-04 | 1.12E-04 | 1.29E-04 | 1.84E-04 | 2.87E-04 | 2.05E-04 | 1.54E-04 | 3.14E-04 |
| Nov | 2.28E-03 | 1.71E-04 | 1.72E-04 | 4.06E-04 | 8.57E-04 | 2.67E-04 | 1.68E-04 | 2.76E-03 |
| Dec | 2.13E-04 | 1.29E-04 | 4.71E-04 | 2.34E-04 | 3.93E-02 | 1.80E-04 | 2.32E-04 | 8.85E-04 |

the geoclimatic factor, we first average the point refractivity gradient values and then we apply (7) to approximate the geoclimatic factor values.

The ITU-R P.453-9 [20] normally recommends seasonal estimation of point refractivity gradient. February to cater for January to March, May to cater for April to June, August to cater for July to September and lastly November for October to December. Our seasonal values are provided in Figure 8(a) with their corresponding geoclimatic factor $K$ values in Figure 8(b). These figures also indicate that for all the regions, the worst month falls in February which is summer apart from Cape Town and Bloemfontein with the worst month being May. In addition to seasonal variability, the geoclimatic factor $K$ also varies with region/climatic types as expected. The results compare well with work done earlier in Durban [6, 16, 21, 22] in which the worst month
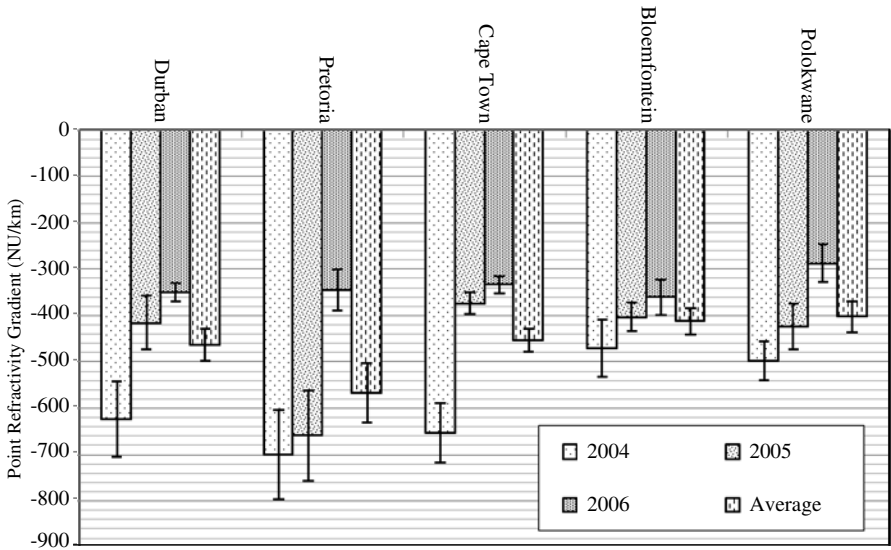
**Figure 7.** Confidence intervals graph for the yearly average of point refractivity gradient for each of the five locations in South Africa.



**Figure 8.** Seasonal variation of (a) point refractivity gradient in the lowest 65 m of the atmosphere not exceeded for 1% of an average year and (b) geoclimatic factor $K$.

for Durban was found to be February followed by August. In [16], where one year radiosonde data is used in the analysis, the average point refractivity gradient was found to be $-572.38$ NU/km. This fits within our confidence interval for the year 2004 for Durban which

**Table 3.** Geoclimatic factor $K$ for Cape Town and Bloemfontein.

| | Cape Town | | | | Bloemfontein | | | |
|---|---|---|---|---|---|---|---|---|
| | 2004 | 2005 | 2006 | Average | 2004 | 2005 | 2006 | Average |
| Jan | 6.35E-04 | 6.44E-04 | 2.24E-04 | 4.51E-04 | 3.32E-04 | 5.92E-04 | 1.48E-04 | 3.08E-04 |
| Feb | 2.71E-03 | 2.18E-04 | 1.17E-04 | 4.11E-04 | 8.39E-05 | 4.32E-04 | 2.66E-04 | 2.13E-04 |
| Mar | 2.00E-04 | 2.56E-04 | 1.64E-04 | 2.03E-04 | 1.24E-04 | 4.90E-04 | 2.99E-04 | 2.63E-04 |
| Apr | 6.17E-04 | 2.32E-04 | 1.61E-04 | 2.84E-04 | 1.20E-03 | 1.21E-03 | 1.61E-03 | 1.33E-03 |
| May | 3.03E-03 | 7.73E-04 | 2.71E-04 | 8.59E-04 | 2.78E-04 | 3.53E-04 | 1.13E-04 | 2.23E-04 |
| Jun | 1.48E-03 | 1.94E-04 | 3.48E-04 | 4.64E-04 | 4.30E-04 | 1.94E-04 | 1.06E-04 | 2.07E-04 |
| Jul | 1.28E-03 | 2.82E-04 | 1.89E-04 | 4.09E-04 | 6.13E-04 | 1.90E-04 | 1.10E-04 | 2.33E-04 |
| Aug | 2.35E-03 | 1.44E-04 | 2.15E-04 | 4.18E-04 | 2.44E-04 | 2.06E-04 | 1.05E-04 | 1.74E-04 |
| Sep | 3.49E-03 | 1.58E-04 | 1.21E-04 | 4.06E-04 | 4.74E-03 | 1.34E-04 | 2.39E-04 | 5.34E-04 |
| Oct | 2.87E-04 | 2.05E-04 | 2.15E-04 | 2.33E-04 | 2.61E-03 | 4.63E-04 | 2.19E-04 | 6.42E-04 |
| Nov | 8.57E-04 | 2.67E-04 | 1.45E-04 | 3.21E-04 | 8.32E-05 | 1.97E-04 | 4.92E-04 | 2.01E-04 |
| Dec | 3.93E-02 | 1.80E-04 | 4.01E-04 | 1.42E-03 | 1.55E-03 | 1.49E-04 | 4.56E-04 | 4.73E-04 |

**Table 4.** Geoclimatic factor $K$ for Polokwane.

| | Polokwane | | | |
|---|---|---|---|---|
| | 2004 | 2005 | 2006 | Average |
| Jan | 1.55E-03 | 4.39E-04 | 1.69E-04 | 4.86E-04 |
| Feb | 1.83E-03 | 1.83E-03 | 6.13E-04 | 1.25E-03 |
| Mar | 1.00E-03 | 6.40E-04 | 3.30E-04 | 5.96E-04 |
| Apr | 1.14E-03 | 1.24E-03 | 7.38E-05 | 4.70E-04 |
| May | 3.71E-04 | 7.92E-04 | 5.01E-04 | 5.28E-04 |
| Jun | 1.85E-04 | 8.08E-04 | 2.11E-04 | 3.16E-04 |
| Jul | 8.46E-05 | 2.72E-04 | 6.54E-05 | 1.15E-04 |
| Aug | 4.47E-04 | 5.92E-05 | 7.99E-05 | 1.28E-04 |
| Sep | 2.95E-04 | 1.45E-04 | 5.65E-05 | 1.34E-04 |
| Oct | 5.00E-04 | 2.26E-04 | 6.58E-05 | 1.95E-04 |
| Nov | 9.82E-04 | 1.17E-04 | 8.56E-05 | 2.14E-04 |
| Dec | 6.48E-04 | 1.41E-04 | 2.94E-04 | 3.00E-04 |

**Table 5.** Comparison of ITU-R and estimated values of point refractivity gradient and geoclimatic factor $K$.

| | Point Refractivity Gradient | | Geoclimatic Factor $K$ | |
|---|---|---|---|---|
| | Mean | Worst Month | Mean | Worst Month |
| Durban | −463.293 | −598.829 (Feb) | 4.48E-04 | 1.04E-03 |
| Cape Town | −453.608 | −475.868 (May) | 4.21E-04 | 4.84E-04 |
| Pretoria | −567.874 | −850.448 (Feb) | 8.58E-04 | 4.97E-03 |
| Bloemfontein | −411.862 | −442.987 (May) | 3.25E-04 | 3.95E-04 |
| Polokwane | −402.688 | −538.205 (Feb) | 3.07E-04 | 7.13E-04 |
| Average | −459.865 | −581.267 | 4.38E-04 | 9.32E-04 |
| **ITU-R** | −400 | | 3.02E-04 | |

ranges from $-705.63$ NU/km to $-541.75$ NU/km (see Figure 7) with an average of $-623.69$ NU/km. However, the succeeding years' values are not within a close range. This seems to confirm our earlier hypothesis that annual variation follow some cycle. In [21], the average point refractivity gradient for Durban was found to be $-523$ NU/km with ten months radiosonde data. The difference in the values is likely due to the size of data used in the analysis and the height resolutions of radiosonde soundings.

Table 5 is a comparison of the estimated values of point refractivity gradient and geoclimatic factor $K$ values with the ITU-R value [20] for Southern Africa. The results imply that the ITU-R value ($-400$ NU/km) under estimates the geoclimatic factor $K$ and it does not consider the worst month situation. Moreover, ITU-R assumes one value of point refractivity gradient for the whole of South Africa, which should never be the case. Geoclimatic factor which is a function of point refractivity gradient is a representative of both topology and climatic conditions of a region. South Africa has more than one climatic type scattered across its regions, hence, it is not a good assumption that it can have one value of point refractivity across all its regions.

## 6.1. Fade Depth and Outage Prediction

The knowledge of fading phenomena is very important in the design and performance of wireless systems. Microwave link attenuation due to multipath is not a permanent occurrence and its probability of occurrence needs to be known for a reliable terrestrial link [2]. It has been mentioned earlier that multipath fading is a random phenomena
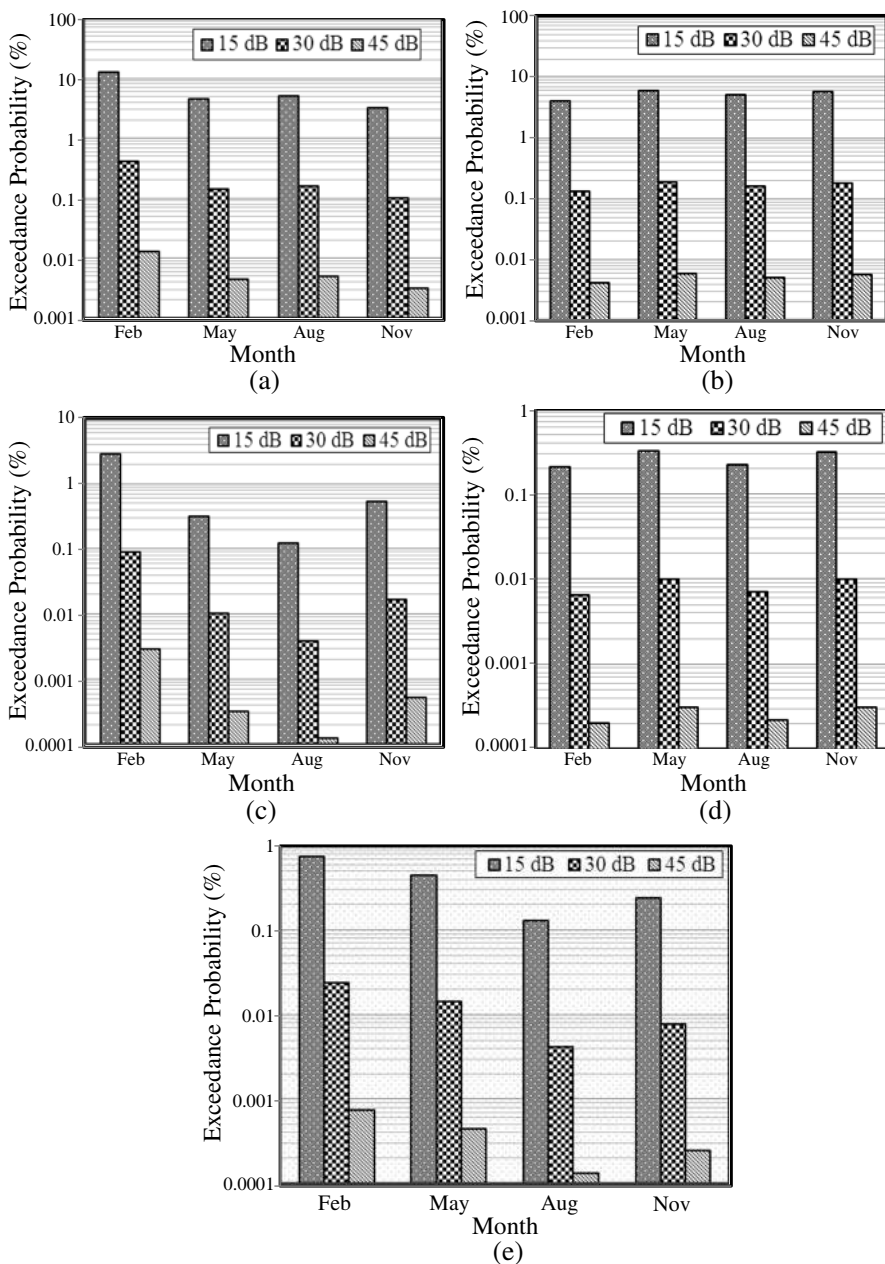
**Figure 9.** Percentage of time a certain fade depth $A$ (dB) is exceeded in (a) Durban, (b) Cape Town, (c) Pretoria, (d) Bloemfontein and (e) Polokwane.

which can only be described statistically. The ITU-R method described in Section 5 is used in estimating the percentage of time that a certain fade depth is exceeded. Prediction of fading phenomena can be made at a fixed value of fade depth or estimated at a certain percentage of outage. The values of geoclimatic factor $K$ as determined in the previous sub-section are used in the prediction of the percentage of time a certain fade depth is exceeded. Equation (9) requires link parameters and in our analysis, we have used the following parameters for the two coastal towns (Durban and Cape Town):

$$f = 11\,\text{GHz},\ h_e = 124\,\text{m},\ h_r = 76\,\text{m and } d = 48.25\,\text{km}.$$

Figure 9(a) shows seasonal variation of the percentage of time various values of fade depth are exceeded for Durban. Figure 9(b) indicates the same for Cape Town. It can be seen that for both cases, the percentage of time that a certain fade depth varies from season to season. For this reason, ITU-R [3] recommends planning around the worst month. In considering the worst month for both the locations, Durban has higher percentages of occurrence than Cape Town even though both are coastal towns. This can be attributed to their difference in climatic types and this stresses the need to determine the geoclimatic factor $K$ for each region for more accurate predictions.

Figures 9(c), (d) and (e) show the probability in percentages, that a certain fade depth is exceeded for Pretoria, Bloemfontein and Polokwane respectively. For these inland locations, the link
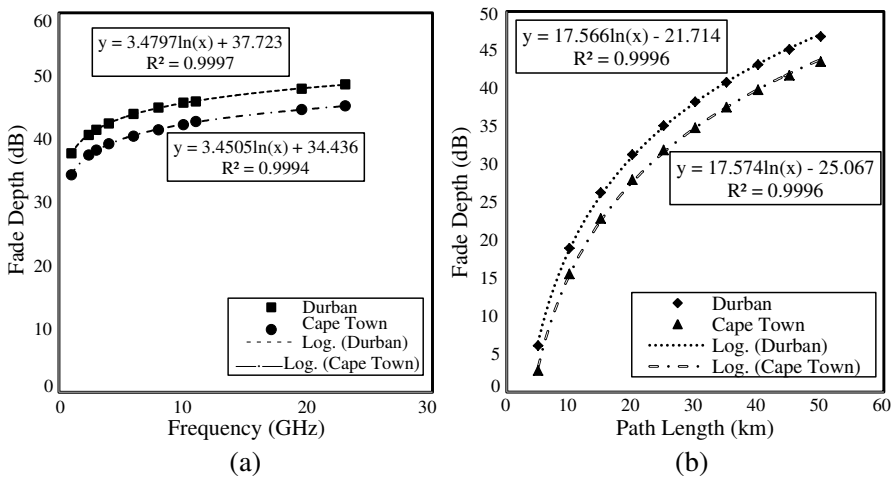


**Figure 10.** Fade depth exceeded for 0.01% of the time (a) with varying frequency at fixed path length (48.25 km) and (b) with varying path length at fixed frequency (11 GHz).

parameters used were adjusted to take their altitudes into effect but still maintaining the path inclination constant as for the coastal towns. This is to make sure that the variation in percentage of time that a certain fade depth is exceeded is due to the geoclimatic factor $K$ of the area. For Durban, Pretoria and Polokwane, the worst month is in February (summer) which compares well with the work of Dabideen et al. [21] in which the highest probability of duct occurrence was found to be in February. ITU-R [20] also confirms the same for the probability of duct occurrence. Duct occurrence has high correlation with multipath fading [21].

In Section 1, the need to determine the fade depth exceeded for 0.01% of the time was explained. Multipath propagation can either result in multipath fading or signal enhancement. The fade depth exceeded for 0.01% of the time is required in predicting system availability for a certain percentage of time [3]. In our study, we determine this value of fade depth exceeded for 0.01% of time with same link parameters as before but with varying frequency as shown in Figure 10(a) at a fixed hop length for both Durban and Cape Town. We again determine this value at a single frequency with varying path length. This is displayed in Figure 10(b). Figure 10(a) shows that the fade depth exceeded increases rapidly with increase in frequency up to about 5 GHz after which the increase is less sharp with increasing frequency. Figure 10(b) shows that path length determines a lot the value of fade depth exceeded for 0.01% of the time. Longer path lengths experience higher values of fade depth exceeded. This can be attributed to the fact that for long distance, multipath is more pronounced because of multiple reflections due to bending of radio beam by the more negative refractivity gradient. The fade depth exceeded for 0.01% of time can be estimated by logarithmic fits with very high coefficient of determination.

## 6.2. Validation and Comparison of Results

The average worst month value for Durban from the three year radiosonde data is used to compare the outage probability with that obtained earlier in Durban by Dabideen e al. [21] and Odedina and Afullo [6]. The first link is between Sherwood and Umlazi in Durban with the following link parameters: $f = 11$ GHz, $h_e = 159$ m, $h_r = 243$ m, and $d = 25$ km. The measured fade depth exceeded for a certain percentage of time, for various link availability is modelled in both ITU-R P530-12 and ITU-R P530-14 models, with geoclimatic factor $K$ as determined as described in the previous sections. These values are compared with values obtained by Dabideen et al. [21], in which they computed their probabilities of exceedance using ITU-R P530-10.

This is shown in Table 6.

The second link is between Howard College Campus and Westville Campus of University of KwaZulu-Natal with the following link parameters: $f = 19.5\,\text{GHz}$, $h_e = 202\,\text{m}$, $h_r = 165\,\text{m}$ and $d = 6.73\,\text{km}$. From the link measurement analysis by Odedina and Afullo [6, 22], the received signal level differs from the expected value of $-41\,\text{dBm}$ by 1–4 dB, which they attribute, could be due to clear air factors when the transmit power is $100\,\text{mW}$ ($20\,\text{dBm}$). The received signal values are far away from the receiver noise level that varies from $-79.5\,\text{dBm}$ to $-82\,\text{dBm}$ [6]. From the mean received signal, the outage probability for the link equals $0.00019\%$ and $0.00014\%$ estimated using ITU-R P530-12 and ITU-R P530-14 respectively. This implies that the average received signal is much higher than the squelch level; therefore the link availability is quite good even with low fade margin. From ITU-R models, $A_{0.01}$ for the link is found to be $19.78\,\text{dB}$ and $18.43\,\text{dB}$ for ITU-R P530-12 and ITU-R P530-14 respectively. The comparison of fade depth for $A_{0.01}$ for the two links confirms that fading due to multipath

**Table 6.** Comparison of fade depth exceeded for various link availability in Durban.

| Outage $p_w$ (%) | Availability (%) | $A_{\text{ITU-R}}$ P530-10 | $A_{\text{ITU-R}}$ P530-12 | $A_{\text{ITU-R}}$ P530-14 |
|---|---|---|---|---|
| 1 | 99 | 16 | 16.22 | 16.4 |
| 0.1 | 99.9 | 26 | 26.22 | 26.4 |
| 0.01 | 99.99 | 36 | 36.22 | 36.4 |
| 0.001 | 99.999 | 46 | 46.22 | 46.4 |
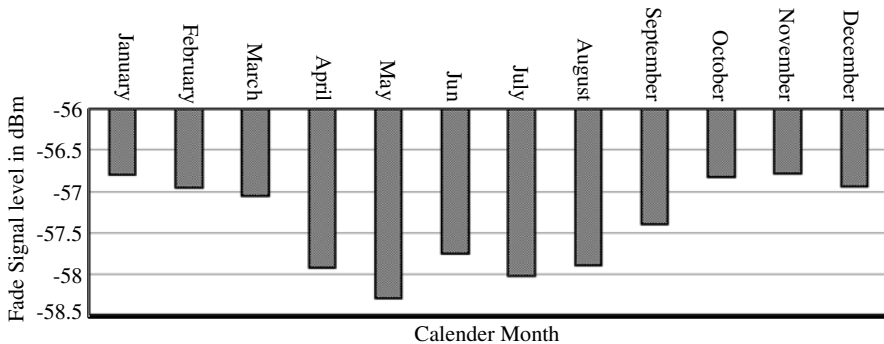


**Figure 11.** Monthly mean received signal level for Jali-Gahengeri link [23].

is more pronounced over long path lengths, as shown in the examples for Rwanda below.

Measurements from three links in Rwanda, Central Africa, are used to estimate outage probability. Average received signal for each month is computed from which fade margin is estimated. This is used in ITU-R models for predicting the probability that a certain fade depth is exceeded in a given link. Table 7 shows typical link parameters and their expected received signal levels. Figures 11–13
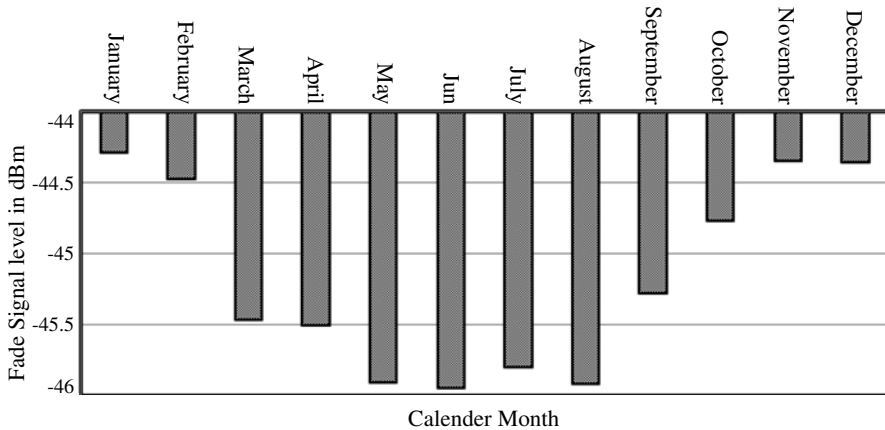


**Figure 12.** Monthly mean received signal level for Gahengeri-Kibungo link [23].
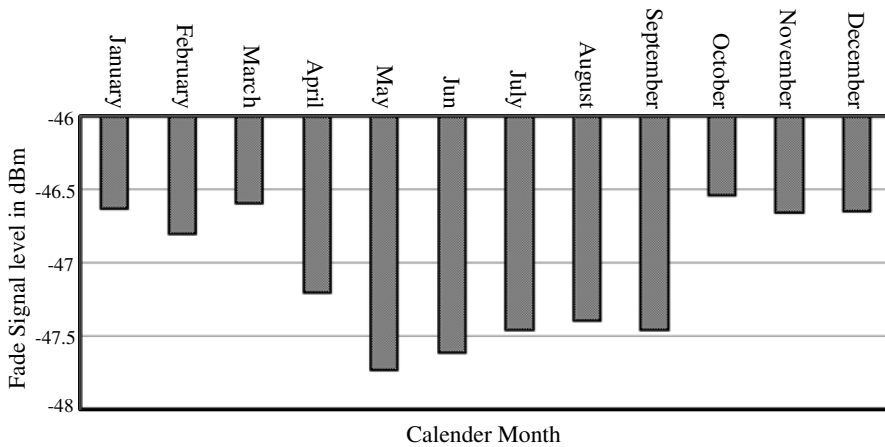


**Figure 13.** Monthly mean received signal level for Nyakarambi-Nasho link [23].

show the monthly mean received signal levels in dBm for each of the links; transmitting power is 0.28 watts (24.5 dBm) in all the cases. The variations in signal levels can be attributed to atmospheric multipath propagation [23].

Djuma [23] used ten year surface measurements data from metrological service from Tanzania bordering Rwanda to estimate point refractivity gradients for four regions. The value for the region closest (Bukoba) to Rwanda was used in estimating outage probabilities for links in Rwanda. The worst month values for various regions are tabulated in the Table 8 below [23]. The worst months are in hot seasons and compares well with South African worst months which are generally in summer months as tabulated earlier in Table 1.

The estimated geoclimatic factor $K$ is used with link parameters in Table 7 to compute the fade depth exceeded for 0.01% of the time. The results are shown in Table 9. They further estimated outage probabilities for the three links by determining the fade margin from mean received value and receiver noise level. Outage occurs when the received signal level is below the receiver noise level. Fade margin levels obtained from link measurements are 13.11 dB, 25.33 dB and 23.46 dB for Jali-Gahengeri, Gahengeri-Kibungo and Nyakarambi-Nasho respectively. Corresponding outage probabilities are also tabulated in Table 9. Receiver threshold noise levels for all the links is $-70.5$ dBm.

**Table 7.** Link parameters [23].

| Link | $d$ (km) | $h_e$ (m) | $h_r$ (m) | $f$ (GHz) | $R_x$ (dBm) |
|---|---|---|---|---|---|
| Jali-Gahengeri | 34.54 | 2084.64 | 1767 | 8 | $-56.57$ |
| Gahengeri-Kibungo | 33.41 | 1663 | 1777 | 8 | $-40.47$ |
| Nyakarambi-Nasho | 17.14 | 1901 | 1764 | 8 | $-42.50$ |

**Table 8.** Point refractivity gradient and geoclimatic factor values for regions in Tanzania.

| | Point Refractivity Gradient | Geoclimatic Factor | |
|---|---|---|---|
| | | ITU-R P530-12 | ITU-R P530-14 |
| Bukoba (Feb) | $-588$ | 3.20E-03 | 9.72E-04 |
| Mwanza (Jan) | $-644$ | 4.65E-03 | 1.38E-03 |
| Kigoma (Dec) | $-589$ | 3.22E-03 | 9.78E-04 |
| Musoma (Mar) | $-901$ | 2.59E-02 | 6.80E-03 |

**Table 9.** Outage probabilities for three links in Rwanda.

|  | $A_{0.01}$ (dB) | |
|---|---|---|
|  | ITU-R P530-12 | ITU-R P530-14 |
| Jali-Gahengeri | 14.06 | 16.05 |
| Gahengeri-Kibungo | 19.52 | 21.74 |
| Nyakarambi-Nasho | < 10 | < 10 |
|  | Outage (%) | |
|  | ITU-R P530-12 | ITU-R P530-14 |
| Jali-Gahengeri | 0.01248 | 0.01971 |
| Gahengeri-Kibungo | 0.00263 | 0.00438 |
| Nyakarambi-Nasho | 0.00018 | 0.00026 |

The above results show that the outage probabilities of the three links in Rwanda are lower than those in Durban with shorter path lengths. This is partly due to lower frequency used in Rwanda and partly due to a more hilly terrain of Rwanda compared to Durban. This can be confirmed by comparing Jali-Gahengeri and Gahengeri-Kibungo links with close link distance. Jali-Gahengeri link which is more hilly (higher surface roughness factor), needs a lower fade margin than for Gahengeri-Kibungo link even though the Gahengeri-Kibungo link used higher gain antennas than the Jali-Gahengeri link. Transmitting/receiving antenna gains used are 41 dBi and 30.8 dBi for Gahengeri-Kibungo link and Jali-Gahengeri link respectively [23].

## 7. CONCLUSION

In this presentation, multipath fading has been examined in relation to the prevailing climatic conditions in five regions of South Africa. Cumulative distribution of refractivity gradient in the lowest 65 m above the ground was determined, from which the point refractivity gradient was estimated. However, in cases where the value was not observable, the Inverse Distance Square (IDS) method has been used to approximate the value. The point refractivity gradient estimated for the regions was found to be more negative than the ITU-R value for South Africa. The ITU-R value of point refractivity gradient for the region is $-400$ NU/km while the estimated value derived from three year radiosonde data was found to be $-459.865$ N units/km. The worst month values of point refractivity gradient for Durban, Pretoria and Polokwane are $-598.829$ NU/km, $-850.448$ NU/km and

$-538.205\,\mathrm{NU/km}$ respectively, all occurring in the month of February. The worst month values point refractivity gradient for Cape Town and Bloemfontein occur in May and are $-475.868\,\mathrm{NU/km}$ and $-442.987\,\mathrm{NU/km}$ respectively. Geoclimatic factor $K$ for the various regions has then been predicted from the various values of point refractivity gradient. It was confirmed that the geoclimatic factor which caters for geographical and climatic conditions in multipath fading distribution varies with the month, season and year. The value is also region based and hence there is need to determine the value for regions of interest for more accurate prediction of fading phenomena. The results also indicate that the worst month varies annually and it generally occurs in the summer months in most of South Africa apart from Mediterranean region (Cape Town) and Steppe region (Bloemfontein) where it occurs in autumn (May). Outage probability in Durban is compared to three links in Rwanda. It's confirmed that even though the geoclimatic factors of the two regions are close, outage probability in Rwanda which is hillier than Durban is lower.

## ACKNOWLEDGMENT

## REFERENCES

1. Grabner, M., V. Kvicera, P. Pechac, and M. Mudroch, "Multipath fading measurement and prediction on 10 GHz terrestrial link," *Proceedings of IEEE 15th Conference of Microwave Techniques*, 2010.

2. Bogucki, J. and E. Wielowieyska, "Empirical season's fading's in radio communication at 6 GHz band," *Journal of Telecommunications and Information Technology*, Vol. 2, 48–52, 2009.

3. ITU-R, "Propagation data and prediction methods required for the design of terrestrial line-of-sight systems," *Recommendation of ITU-R P.530-14,* Geneva, 2012.

4. Olsen, R. L., T. Tjelta, L. Martin, and B. Segal, "Worldwide techniques for predicting the multipath fading distribution on terrestrial LOS links: Comparison with regional techniques," *IEEE Transactions on Antennas and Propagation*, Vol. 51, No. 1, January 2003.

5. Olsen, R. L. and T. Tjelta, "Worldwide techniques for predicting the multipath fading distribution on terrestrial LOS links:

Background and results of tests," *IEEE Transactions on Antennas and Propagation,* Vol. 47, No. 1, January 1999.

6. Odedina, P. K. and T. J. Afullo, "Clear air signal level measurements for microwave line-of-sight link application in South Africa," *SAIEE Transactions*, Vol. 101, No. 4, 132–139, December 2010.

7. Adediji, A. T. and M. O. Ajewole, "Vertical profile of radio refractivity gradient in Akure, south-west Nigeria," *Progress In Electromagnetic Research C,* Vol. 4, 157–168, 2008.

8. Tjelta, T., et al., "Correlation of observed multipath occurrence with climatic parameters derived from radiosondes, surface stations, and numerical models," *CLIMPARA*, 85–92, Ottawa, Canada, April 27–29, 1998.

9. http://www.sa-venues.com/no/weather.htm.

10. Fashuyi, M. O., "A study of rain attenuation on terrestrial paths at millimetric wavelengths in South Africa," Ms.c. Thesis, University of KwaZulu-Natal, 2006.

11. Fashuyi, M. O., P. A. Owolawi, and T. J. O. Afullo, "Rainfall rate modelling for LOS radio systems in South Africa," *Transactions of South African Institute of Electrical Engineers (SAIEE),* Vol. 97, No. 1, 74–81, March 2006.

12. http://www.bdb.co.za/kimberley/climate.htm.

13. Lystad, S. L., et al., "Interpolation of clear air parameters observed at non-regular observation locations," *CLIMPARA*, 15–26, Ottawa, Canada, April 27–29, 1998.

14. Li, J. and A. D. Heap, *A Review of Spatial Interpolation Methods for Environmental Scientists*, 137, Geoscience Australia, Record 2008/23, ISBN 978-1-921498-282.

15. Freeman, R. L., *Radio System Design for Telecommunications*, John Wiley & Sons, 1997, ISBN 978-0-471-75713-9.

16. Odedina, P. K. and T. J. Afullo, "Use of spatial interpolation technique for determination of geoclimatic factor and fade depth calculation in Southern Africa," *Proceedings of IEEE AFRICON Conference*, Windhoek, Namibia, September 26–28, 2007.

17. Abu-Alman, A. and K. Al-Ansari, "Calculation of effective earth radius and point refractivity gradient in UAE," *International Journal of Antennas and Propagation*, Vol. 2010, 1–4, doi. 10.1155/2010/245070.

18. Odedina, P. K. and T. J. Afullo, "Estimation of secondary radioclimatic variables and its application to terrestrial LOS link design in Southern Africa," *Proceedings of IEEE AFRICON*

*Conference*, Wild Coast Sun, South Africa, September 7–10, 2008.

19. Al-Ansari, K. and R. A. Kamel, "Correlation between ground refractivity and refractivity gradient and their statistical and worst month distribution in Abu Dhabi," *IEEE Antennas and Wireless Propagation Letters*, Vol. 2, 233–235, 2008.

20. ITU-R, "The radio refractivity index: Its formula and refractivity data," *Recommendation of ITU-R P.453-9,* Geneva, Switzerland, 2003.

21. Dabideen, A. S., M. Gopichund, and T. J. Afullo, "Radio refractivity distribution and duct and fading occurrence measurements in kwazulu-natal," *Transactions of South African Institute of Electrical Engineers (SAIEE)*, Vol. 96, No. 2, 121–132, June 2005.

22. Odedina, P. K. and T. J. Afullo, "Multipath propagation modeling and measurement in a clear-air environment for LOS link design application," *Southern Africa Telecommunication Networks and Applications Conference Proceedings*, Ezulwini Swazi, Royal Spa, Swaziland, August 31–September 2, 2009.

23. Djuma, S., "Clear-air microwave signal prediction on terrestrial paths in Central Africa using existing models," Ms.c. Thesis, National University of Rwanda, September 2012.